DOI: ADD DOINUMBER HERE

Sensitivity Analysis Study of Expanding Hypersonic Flows of Nitrogen and Oxygen

Oblapenko Georgii[⋆†] *and Hannemann Volker*[⋆]
[⋆]*German Aerospace Center (DLR)*
Bunsenstrasse 10, 37073 Göttingen, Germany
georgii.oblapenko@dlr.de · volker.hannemann@dlr.de
[†]Corresponding author

Abstract

Sensitivity analysis studies of expanding high-enthalpy binary flows of nitrogen and oxygen in hypersonic nozzles are carried out for a variety of conditions. The polynomial chaos expansion (PCE) methodology is utilised to assess the sensitivity of the free-stream conditions to vibrational and chemical relaxation rates, as well as the reservoir conditions. It is shown that for high-enthalpy conditions, the main contributors to uncertainty in the free-stream flow are uncertainties in the vibrational and chemical relaxation rates for molecule-atom collisions, as well as uncertainties in the reservoir conditions. The impact of high-temperature vibrational relaxation time corrections and the vibrational-chemical coupling was found to be negligible for the investigated cases. A preliminary analysis on the potential influence of ionization was also performed, which was found to have an insignificant effect on the free-stream conditions in nitrogen.

1. Introduction

Expanding hypersonic flows are widely used in ground test facilities to achieve conditions similar to those of high-velocity hypersonic re-entry in order to provide experimental data for spacecraft design. Simulations of such flows are required for an estimation of the ground test facility free-stream conditions; however, the numerical computation of high-enthalpy flows is complicated by the significant number of relaxation processes (internal energy transitions, chemical reactions) that need to be considered. Data (experimental or quasi-classical trajectory computation-based) on the rates of these processes can be subject to significant uncertainties, which lead to existence of uncertainties in the computed flow properties. The choice of computational models describing the relaxation processes can also have a strong effect on the numerical solution;[11,12,18,26,33] however, given the strong focus on accurately simulating flows behind strong shock waves (such as those occurring during re-entry processes), some widely used computational models have been extensively tested for high-enthalpy compression flows, but their applicability to expansion flows remains questionable.[5,12,20,30] Given the presence of uncertainties in reaction rates and the choice of computational models to describe thermochemical relaxation, there has been a growing interest in understanding the impact of these uncertainties on high-speed high-enthalpy flow modeling. Most of the effort has been focused on flows behind strong shock waves,[2,7,16,17,39–41,43] and expanding flows, such as those occurring in high-enthalpy experimental facilities, have received less attention, despite there often being discrepancies between simulation results and experimental data.[8,13,15,24,27,29,32,42] Several recent studies have focused on improvement of modeling of expanding flows in experimental facilities: in Gimelshein & Wysong,[10] the impact of chemical reaction rates on nitric oxide production was studied, along with the role of variations in the reservoir density and temperature; and in Gu et al.,[12] the applicability of two-temperature models (as compared to higher-fidelity state-specific models) to simulations of nozzle flow was investigated, along with the possibility of simplification of vibrational relaxation modeling in air flows.

The present work has the following objectives. The first is to establish the computational methodology, discuss the underlying assumptions, and provide an analysis of uncertainties in thermochemical relaxation rates. The second is a quantitative study of the influence of uncertainties in the non-equilibrium process rate data and choice of computational models on high-enthalpy expanding flow modeling for several selected conditions. This will allow for a clearer picture on the applicability of various modeling assumptions, and provide detailed information on the main sources of uncertainty in the flow, which can be used as a basis for experiment design or QCT computations in order to obtain better relevant thermochemical relaxation data. The final objective is to provide better defined uncertainty bounds for free-stream conditions in high-enthalpy experimental facilities, in order to aid further uncertainty quantification and

sensitivity studies of re-entry flows around blunt bodies. Whilst the present work focuses on binary flows of nitrogen and oxygen, the aim is also to utilize the results as a basis for future studies of expanding air flows.

1.1 Governing Equations

In the present work, we assume a steady inviscid quasi-one-dimensional flow through a nozzle, the axis of which is aligned with the x coordinate direction. Thus, within the multi-temperature approach, the system of the governing flow equations can be written out as follows:

$$\frac{d\left(\rho_c v S\right)}{dx} = S R_c^{chem},\ c = 1, \ldots, N_s, \tag{1}$$

$$\rho v \frac{dv}{dx} = -\frac{dp}{dx}, \tag{2}$$

$$\frac{dh}{dx} + v\frac{dv}{dx} = 0, \tag{3}$$

$$\frac{d\left(S v E_v^c\right)}{dx} = S R_c^{vibr},\ c = 1, \ldots, N_m. \tag{4}$$

Here ρ_c is the density of chemical species c, v is the flow velocity along the nozzle axis, x is the length along the axis, $S = S(x)$ is the cross-section area of the nozzle, N_s is the overall number of chemical species in the flow, p is the pressure, h is the flow enthalpy, E_v^c is the vibrational energy per unit mass of molecular species c, N_m is the number of molecular species in the flow, and R_c^{chem} and R_c^{vibr} are the chemical and vibrational relaxation terms, respectively. Viscous effects are not investigated in the present work, because their influence on the expansion core flow is small. A boundary layer correction could enter the numerical setup via an en effective nozzle contour $S(x)$.

Since at this stage of the investigation we only consider binary mixtures, the VV-exchange of vibrational energy between molecules are not taken into account, as they are a rapid process.[23] Thus, the vibrational relaxation term R_c^{vibr} describes the overall change of vibrational energy of species c due to VT exchanges between vibrational and translational modes $R_c^{vibr,VT}$, and vibrational energy loss/gain due to dissociation/recombination reactions $R_c^{vibr,chem}$:

$$R_c^{vibr} = R_c^{vibr,VT} + R_c^{vibr,chem}. \tag{5}$$

In the present work, the VT relaxation is described the Landau–Teller relaxation equation:

$$R_c^{vibr,VT} = \rho_c \frac{E_v^c(T) - E_v^c(T, T_v^c)}{\tau_c^{VT}}, \tag{6}$$

where τ_c^{VT} is the VT relaxation time of molecular species c and T_v^c is the vibrational temperature of the species.

In a binary flow, where only dissociation–recombination reactions take place, the chemical reaction term for atomic species is directly expressed via the chemical reaction term for the molecular species: $R_{at}^{chem} = -R_{mol}^{chem}$, where the chemical relaxation term for molecular species is computed as follows:

$$R_{mol}^{chem} = m_{mol} n_{at}^2 \sum_d n_d k^{rec,cd}(T) - m_{mol} n_{mol} \sum_d n_d k_{cd}(T, T_v^c), \tag{7}$$

where $k_{cd}(T, T_v^c)$ is the rate coefficient of a dissociation reaction during a collision of molecular species c with chemical species d, and $k^{rec,cd}$ is the corresponding reverse (recombination) rate coefficient.

The chemical relaxation processes in the present work are treated using the Park[28] and Treanor–Marrone[22] models for dissociation reaction rates. The Park model gives the multi-temperature reaction rate in the following form:

$$k_{cd}(T, T_v^c) = A T_{eff}^n \exp\left(-\frac{E_c}{k T_{eff}}\right), \tag{8}$$

where E_c is the reaction's activation energy, A and n are the Arrhenius law coefficients, and $T_{eff} = T^s \left(T_v^c\right)^{1-s}$ is the effective temperature, governed by a reaction-specific constant s, which quantifies the degree of vibration-chemical coupling. s is usually taken to be 0.5 for dissociation reactions in expanding flows.

The Treanor–Marrone model gives the following expression for the state-specific dissociation reaction rates (rate of dissociation from vibrational level i):

$$k_{cd,i}^{diss}(T) = Z_i(T) k_{cd}^{diss,eq}(T), \tag{9}$$

where $k_{cd}^{diss,eq}(T)$ is the equilbrium reaction rate coefficient and the non-equilibrium factor $Z_i(T)$ is given by the following expression:

$$Z_i(T) = \frac{Z_v^c(T)}{Z_v^c(-U_{TM})} \exp\left(\frac{\varepsilon_i}{k}\left(\frac{1}{T} + \frac{1}{U_{TM}}\right)\right). \tag{10}$$

Here Z_v^c is the equilibrium (Boltzmann) partition function, ε_i is the vibrational energy of level i of the dissociating molecule, and $U_{TM} = U_{TM}(T)$ is an adjustable parameter, that describes the degree of preferential dissociation from higher-lying vibrational levels. In order to obtain the multi-temperature rate $k_{cd}(T, T_v^c)$, the state-specific rates are averaged over the vibrational distribution:

$$k_{cd}(T, T_v^c) = \sum_i k_{cd,i}^{diss}(T) x_{ci}(T, T_v^c), \tag{11}$$

where x_{ci} is the fraction of molecules which are in vibrational state i.

The backward reaction (recombination) rates are computed using equilibrium constants.

2. Uncertainty Quantification and Sensitivity Analysis

In order to assess the impact of the uncertainties in the reservoir parameters and thermochemical relaxation rates on the flow, the generalized Polynomial Chaos (gPC)[35] method is utilised. Denoting the vector of uncertain model parameters as $\mathbf{w}$, and assuming that all these uncertain parameters are independent random variables, a quantity of interest Y (such as pressure, temperature, etc.) can be represented in the following form:

$$Y(x, \mathbf{w}) \approx \sum_{i=0}^{N} c_i(x) P_i(\mathbf{w}). \tag{12}$$

Here $c_i(x)$ are the unknown expansion coefficients (which are dependent on the spatial location x), and P_i are the expansion polynomials (of order i up to N), which are known beforehand and are chosen to be orthogonal with respect to the parameter distributions. Due to the orthogonality of the polynomials, the coefficients of the expansion are given through the following expression:

$$c_i = \frac{\langle Y, P_i \rangle}{\langle P_i, P_i \rangle}, \quad \langle a, b \rangle = \int abd\mathbf{w}. \tag{13}$$

Once the set of uncertain model parameters $\mathbf{w}$ and their distributions have been chosen, along with the desired order of the polynomial expansion N the quadrature appearing in Eqn. 13 can be evaluated numerically. For a chosen quadrature rule, a set of sample points of $\mathbf{w}$ is generated, along with the associated weights, the model is evaluated using the sampled values of the uncertain parameters, and the quadrature is calculated in order to obtain the coefficients c_i. Smolyak sparse grids are used for evaluation of the quadrature in order to reduce the number of model evaluations required. In the present work, 3^{rd} order polynomial expansions are used, as they were found to provide sufficient convergence of the statistical properties being investigated (mean, standard deviation, sensitivity indices). Once the expansion coefficients c_i have been computed, relevant statistics can be calculated, such as the mean and standard deviation of the flow quantities of interest (for example, temperature at the nozzle exit), as well as the sensitivity of these flow quantities with respect to the uncertain model parameters (via Sobol sensitivity indices). The total Sobol sensitivity index of quantity of interest Y with respect to uncertain model variable w_i is defined as

$$S_{tot,i} = 1 - \frac{\mathrm{Var}_{\mathbf{w}_{\sim \mathbf{i}}}\left(E_{w_i}\left(Y|\mathbf{w}_{\sim \mathbf{i}}\right),\right)}{\mathrm{Var}(Y)} \tag{14}$$

where Var is the variance, E is the expectation, and $\mathbf{w}_{\sim \mathbf{i}}$ is the vector of all uncertain model variable except variable w_i.

The following sources of model uncertainty are considered in the present study: reservoir conditions, vibrational relaxation rates, chemical relaxation rates, and the degree of vibrational-chemical coupling. In addition, for the high-enthalpy nitrogen simulations, the potential role of ionization and electron-impact vibrational relaxation is considered, albeit in an inexact fashion. For the reservoir conditions (reservoir temperature T_r and reservoir pressure p_r), an uncertainty range of ±2.5% (around a given mean value) is assumed. For the vibrational relaxation rates, three uncertain parameters are considered: two parameters governing the VT relaxation time in molecule-molecule and molecule-atom collisions, correspondingly, as well as a parameter governing the degree of the high-temperature Park correction applied to the VT relaxation times. The parametrization of the VT relaxation times used in the present study was performed as follows. The Millikan–White model was used for the computation of the VT relaxation times; for each collision of molecular species c with chemical species d, the VT relaxation time is governed by two parameters A_{cd} and B_{cd}:

$$p\tau_{cd}^{VT} = \exp\left(A_{cd}\left(T^{-1/3} - B_{cd}\right) - 18.42\right). \tag{15}$$

While the A_{cd}, B_{cd} coefficients can be varied independently, doing so may lead to uncharacteristically low or high values of the VT relaxation times. Thus, in the present work, these coefficients are taken to be linearly dependent on a model parameter $\alpha_{VT,cd}$:

$$A_{cd} = A_{cd}^{(0)} + A_{cd}^{(1)}\alpha_{VT,cd}, \quad B_{cd} = B_{cd}^{(0)} + B_{cd}^{(1)}\alpha_{VT,cd}. \tag{16}$$

The single uncertain parameter $\alpha_{VT,cd}$ is taken to be uniformly distributed between 0 and 1, and the coefficients of the linear dependencies in Eqn. 16 are chosen based on analysis of existing experimental and QCT data for VT relaxation times. The use of a single parameter (instead of two) also allows for a reduction in the parameter space dimensionality, lowering the number of model evaluations required.

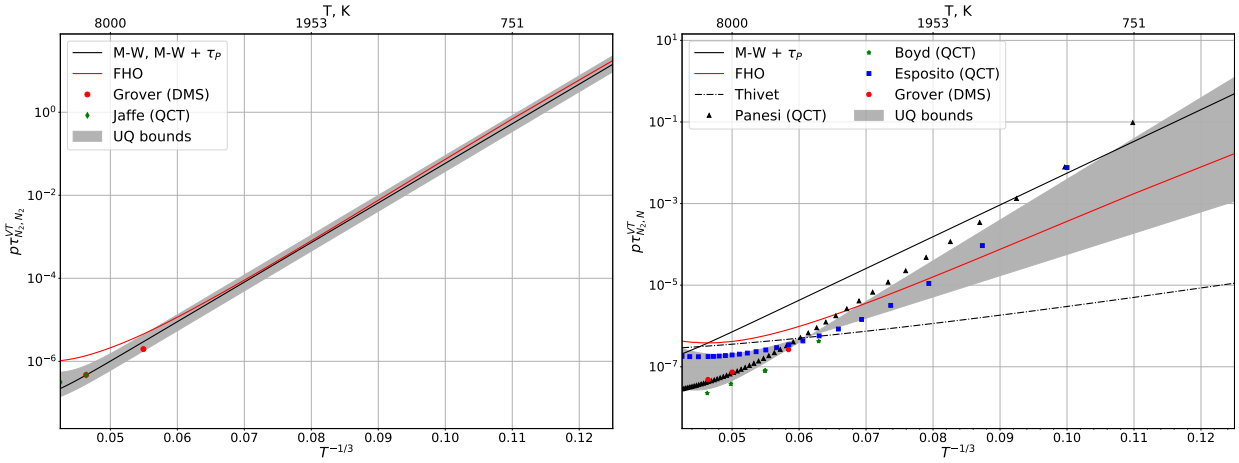

Figure 1: Pressure-corrected VT relaxation times of nitrogen molecules in collision with nitrogen molecules (left) and atoms (right).

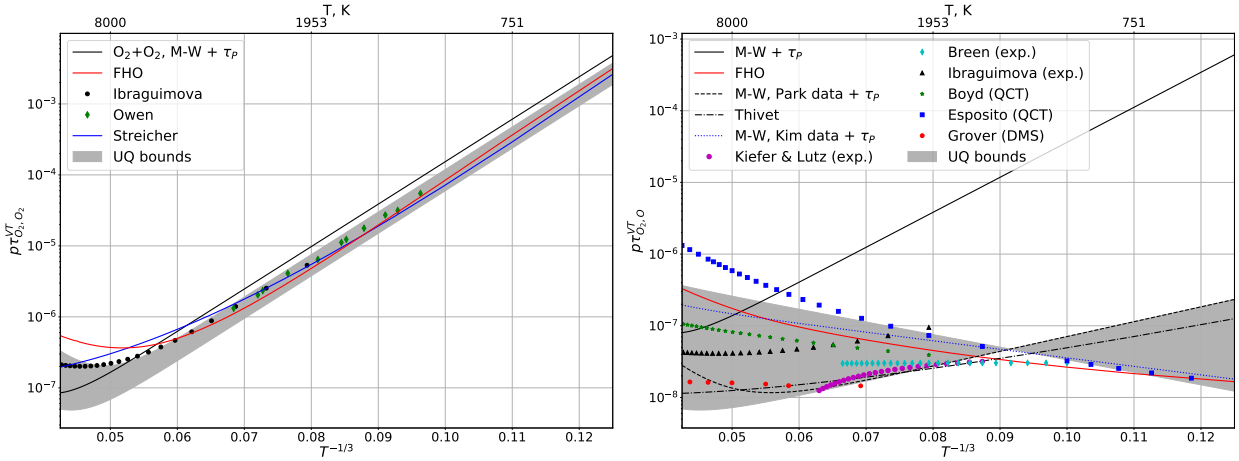

Figure 2: Pressure-corrected VT relaxation times of oxygen molecules in collision with oxygen molecules (left) and atoms (right).

Fig. 1 shows the vibrational relaxation times of N_2 colliding with N_2 (left) and N (right) compiled from a variety of literature sources, which include both experimental data and quasi-classical trajectory computations. The shaded grey region denotes the range of vibrational relaxation times covered in the present work as α_{VT} is varied from 0 to 1. Fig. 2 shows the vibrational relaxation times of O_2 colliding with O_2 (left) and O (right). The O_2–O_2 vibrational relaxation times are well-studied experimentally, and recent experimental data (and associated curve fits) are presented, which show a low degree of discrepancy in the considered temperature range. For O_2-O collisions, the picture is far less

clear, with the data not only differing significantly at higher temperatures, but also exhibiting different monotonicity. Recent uncertainty quantification studies of QCT-derived vibrational relaxation times in O_2-O collisions also noted large difference between results obtained through the use of different potential energy surfaces.[38] Given the high degree of variance present in the data, the low values of the relaxation times, and the high degree of dissociation of oxygen in high-enthalpy flows, it can be expected that the uncertainties in VT relaxation rates in O_2-O collisions will have a noticeable impact on the relevant flow properties. For a more detailed overview of vibrational relaxation times in air mixtures, the reader is referred to.[25]

Finally, since at high temperatures the Millikan–White expression underestimates the VT relaxation times, a correction time proposed by Park is usually added to the relaxation times. This VT relaxation correction is dependent on an adjustable cross-section parameter σ_{cd}. In the present work, σ_{cd} is taken to be in the form $\sigma_{cd} = \sigma_{cd,0}10^{\sigma_P}$, where σ_P is the uncertain model parameter, assumed to be uniformly distributed between 0 and 1.

For the case of the high-enthalpy nitrogen flow, in order to estimate the potential impact of ionization on the vibrational temperature (due to the fast vibrational relaxation of molecules in collisions with electrons), the following methodology is used. Given the pressure p and temperature T, the equilibrium electron number density is computed based on Saha's equation.[1] Based on this number density, the vibrational relaxation time due to N_2-e collisions is computed via the approximation of Lee,[21] assuming that the electron temperature T_e is equal to the vibrational temperature of nitrogen. Therefore, whilst such an approach is not fully consistent, as it does not model the actual ionization and all relevant collisional and convective processes throughout the domain, it can provide a rough estimate for the potential role of ionization in the flow. In order to quantify the role of the electron-nitrogen collisions on the flow, the computed electron number density n_e is scaled by a factor $\alpha_{VT,e}$, which is assumed to be uniformly distributed between 0 and 4. Thus, the "effective" electron number density is varied from 0 to 4 times the equilibrium number density, in order to cover a wider range of possible electron number densities.

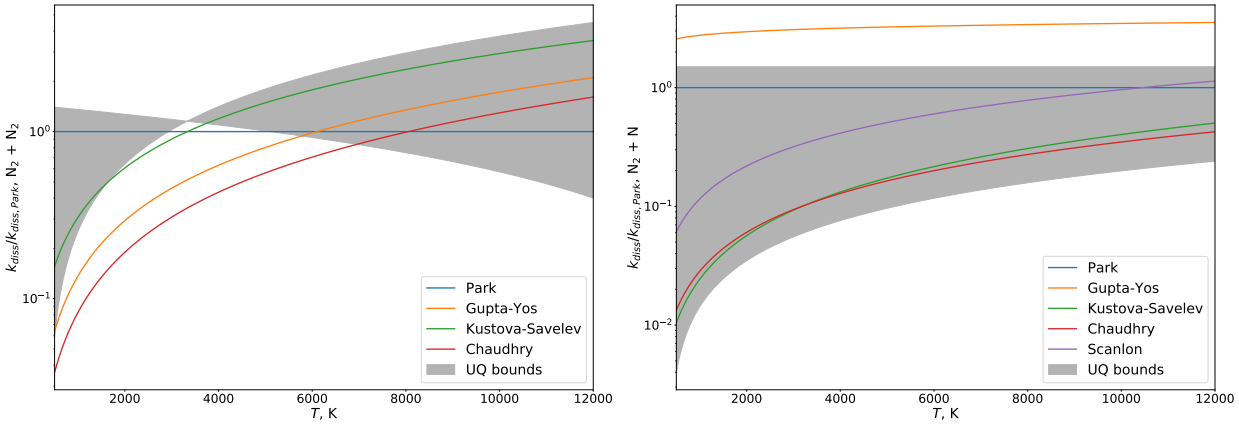

Figure 3: Ratio of k_{diss} computed using different Arrhenius model constants to k_{diss} computed using Park's data for dissociation of N_2 in collisions with N_2 (left) and N (right).

For the chemical relaxation rates, three parameters were considered: two parameters governing the equilibrium dissociation rate coefficients in molecule-molecule and molecule-atom collisions, and a parameter governing the degree of vibrational-chemical coupling. A similar approach was taken to the variation of the equilibrium dissociation rate coefficients as to the variation of the VT relaxation times, both in order to reduce the dimension of the parameter space and to avoid uncharacteristically low or high values of the reaction rates. The reaction rates were assumed to be in the form

$$k_{cd}^{diss}(T) = (a_{cd}^{diss} + b_{cd}^{diss}T)k_{cd,Park}^{diss}(T), \tag{17}$$

where $k_{cd,Park}^{diss}(T)$ are the equilibrium dissociation rate coefficients computed on the basis of data given by Park.[28] The coefficients a_{cd}^{diss}, b_{cd}^{diss} were taken to be linearly dependent on a model parameter $\alpha_{diss,cd}$, which was assumed to be uniformly distributed between 0 and 1. Thus, by varying $\alpha_{diss,cd}$, one can "sweep" through a range of values of the dissociation rate coefficient; the ranges were chosen based on analysis of existing reaction rate data. Figure 3 shows the ratio of equilibrium dissociation rates of nitrogen computed on the basis of various data to the rates computed using the data of Park, with the grey region covering the range of values considered in the present work. Apart from the Park data, the data considered includes the widely used datasets of Gupta and Yos[14] and Scanlon et al.,[31] as well as the recent QCT-based data of Kustova and Savelev,[19] and Chaudhry and Candler.[4] For oxygen dissociation, the recent experimental data of Streicher et al.[36] is also included, shown on Fig. 4.

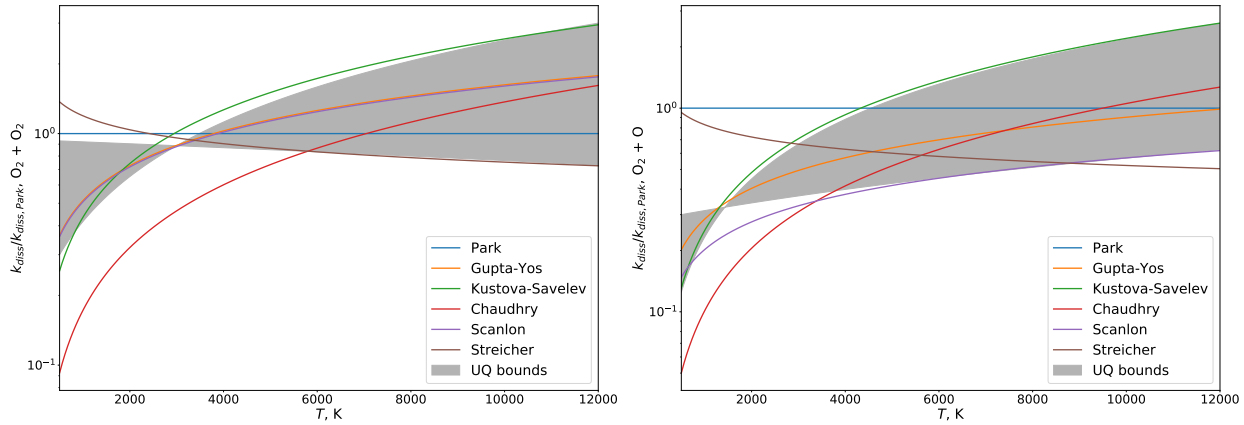

Figure 4: Ratio of k_{diss} computed using different Arrhenius model constants to k_{diss} computed using Park's data for dissociation of O_2 in collisions with O_2 (left) and O (right).

Finally, the parameter governing the degree of vibrational-chemical coupling needs to be considered. For the case of the Park model, the parameter s appearing in the expression for the effective reaction temperature was varied between 0.5 and 1. For computations performed using the Treanor–Marrone model the parameter U_{TM} was varied via a parameter α_U. The functional form of U_{TM} is taken to be

$$U_{TM}(T) = U_{TM}^{(0)} + U_{TM}^{(1)} T, \tag{18}$$

where $U_{TM}^{(0)}$ and $U_{TM}^{(1)}$ are temperature-independent coefficients. As for the VT relaxation times and chemical relaxation rates, these coefficients were taken to have a linear dependence on the parameter α_U (which varies from 0 to 1 and is uniformly distributed), so that if $\alpha_U = 0$, $U_{TM} = D/6k$ (where D is the dissociation energy of the molecular species considered), and if $\alpha_U = 1$, $U_{TM} = 3T$. Thus, two commonly used values of the Treanor–Marrone model parameter (one temperature-dependent, one temperature-independent) are reproduced, as well as various in-between values.

Thus, 8 uncertain parameters in total are considered in the present work (2 reservoir conditions, 3 parameters governing vibrational relaxation, 3 parameters governing chemical relaxation). For the computations that included the electron-impact vibrational relaxation, the parameter governing the degree of vibrational-chemical coupling was replaced by the parameter $\alpha_{VT,e}$. For 8 uncertain parameters and the 3^{rd} order polynomials considered in the present work, 849 model evaluations were required in order to compute the expansion coefficients and the statistical properties of the quantities of interest.

3. Numerical Results

We consider two different flow conditions. The first is based on the experiments of Sharma et al.[32] in the NASA EAST facility. The experiments were performed in a nitrogen flow through a 8.3 cm nozzle; the reservoir pressure and reservoir temperature were 10.13 MPa and 5600 K, correspondingly. The second flow condition is based on the HEG shock tunnel condition H22R0.20 (a reservoir pressure of 35 MPa and reservoir temperature of 9100 K) through a 3.78 m contoured nozzle (Nozzle 5).[15] For the first flow condition, a binary flow of nitrogen was considered; for the second flow condition, binary flows of both nitrogen and oxygen were considered. The choice of the NASA EAST test case condition was motivated by the availability of experimental measurements of the vibrational temperature and a pre-computed effective nozzle profile (based on 2-dimensional viscous computations). The choice of the HEG H22R0.20 condition was motivated by the high enthalpy (and therefore, stronger influence of thermochemical relaxation rates compared to the NASA EAST test case), as well the aim of the present work to prepare a basis for future studies in air flows, for which experimental data from the HEG shock tunnel is available. For all flows, based on the statistical analysis of multiple simulations (which vary in the relaxation rates and the reservoir conditions), the mean and standard deviation of the flow quantities of interest (translational and vibrational temperatures, pressure, velocity, and molar fraction of molecules) were calculated, along with the Sobol total sensitivity indices for the values of these flow quantities at the nozzle exit. The Chaospy[9] Python library was used to sample the values of the uncertain parameters and perform the post-processing (computation of the uncertainties and sensitivity indices). Thermochemical equilibrium was assumed in the reservoir, and from the computed enthalpy and entropy the nozzle throat conditions were calculated (also assuming thermochemical equilibrium); these were used as the initial conditions for the 1-D solver.

3.1 NASA EAST Expansion

First, we consider the condition corresponding to the experiments performed in nitrogen in the NASA EAST facility.[32] The Treanor–Marrone model was used for the simulations. As very little reactions occur in the flow due to the relatively low enthalpy, a comparison between different vibration-dissociation coupling models was not carried out for these conditions.

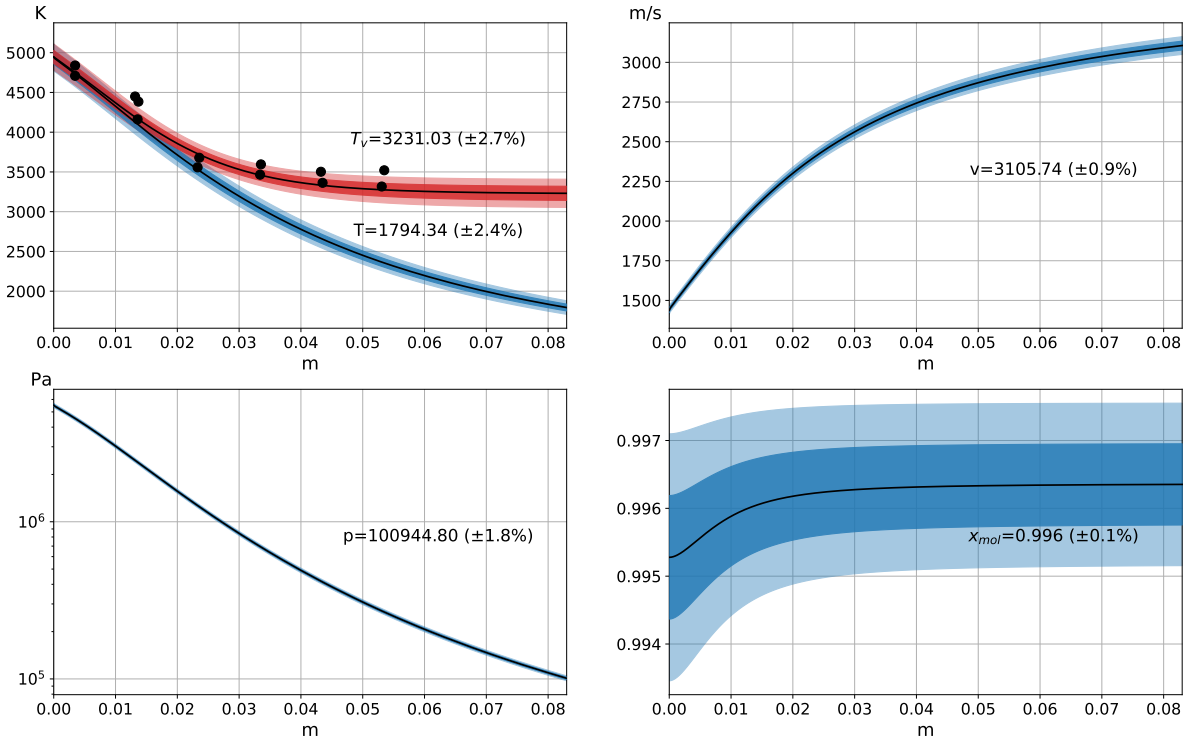

Figure 5: Profiles of temperatures, velocity, pressure, and molecular molar fraction along the nozzle axis. Flow of nitrogen through NASA EAST nozzle. Values at nozzle exit expressed explicitly.

Figure 5 shows the flow properties (temperature, vibrational temperature, velocity, pressure, and molar fraction of molecules) computed along the nozzle axis between the nozzle throat (located at $L = 0$ m) and nozzle exit (located at $L = 0.083$ m). Black circles denoted the experimental measurements. Black lines denote the computed mean values, and the shaded regions denoted a range of ± one standard deviation. Values of the flow properties at the nozzle exit are annotated on the subplots along with the associated uncertainties (the computed standard deviations of the values). It can be seen that for the relatively low-enthalpy condition considered (7.3 MJ/kg), the temperatures and pressure exhibit the strongest variation, whereas the chemical composition of the flow barely changes. A reasonable agreement is obtained with the experimental data; moreover, the degree of uncertainty in the reservoir pressure (±2.5%) that is assumed in the present study might be somewhat lower than that observed in the experiments.

Figure 6 shows the total Sobol sensitivity indices of the flow properties (temperature T, vibrational temperature of nitrogen T_v, velocity v, pressure p, molar fraction of nitrogen molecules x_{mol}, and degree of vibrational non-equilibrium as quantified by the difference $T_v - T$) at the nozzle exit with respect to the uncertain model parameters: the reservoir pressure p_r and temperature T_r, the two parameters governing vibrational relaxation times for molecule-molecule and molecule-atom collisions ($\alpha_{VT,mm}$, $\alpha_{VT,ma}$), the cross-section σ_P for the Park high-temperature VT relaxation time correction,[28] the two parameters governing the dissociation rates in molecule-molecule and molecule-atom collisions ($\alpha_{diss,mm}$, $\alpha_{diss,ma}$), and the parameter α_U governing the value of the quantity U_{TM} used to describe the vibration-dissociation coupling in the Treanor–Marrone model. Sensitivities with respect to the reservoir conditions are denoted by the orange bars, with respect to the vibrational relaxation parameters with blue bars, and with respect to the chemical relaxation parameters with green bars. The sensitivity indices are dimensionless quantities which quantify the relative sensitivities of the quantities of interest with respect to the uncertain model parameters, accounting for higher-order interactions between them. Higher values of the indices correspond to higher sensitivities. It should be noted that the Sobol sensitivity indices are plotted on a log scale, and one can see that the relative influence of the different parameters on the flow at the nozzle exit can vary up to several orders of magnitude. Under the conditions considered,

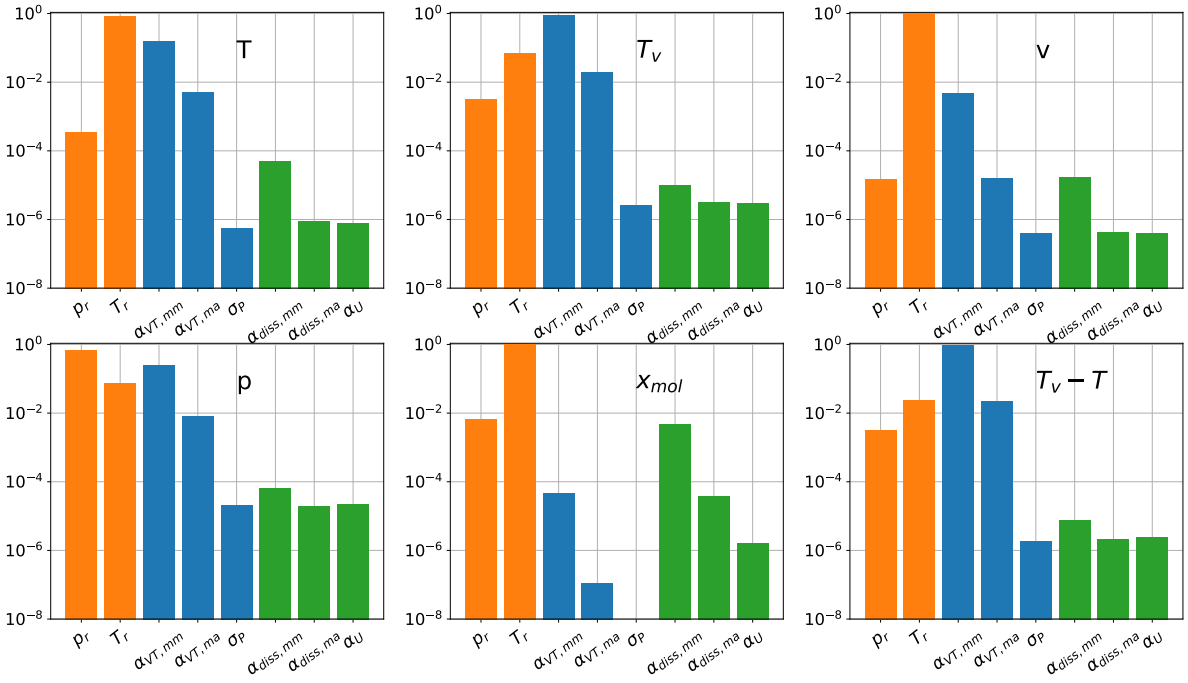

Figure 6: Total Sobol sensitivity indices of flow parameters at nozzle exit with respect to uncertain model parameters. Flow of nitrogen through NASA EAST nozzle.

where temperatures are relatively low, and chemical reactions do not play a significant role, the main influence on the flow parameters is from the reservoir conditions and the vibrational relaxation times. Despite the low molar fraction of atomic nitrogen, due to the significantly lower VT relaxation times for N_2-N collisions (as seen on Fig. 1), their influence on the temperatures is still present. As expected, the choice of the Park correction factor has virtually no influence on the flow due to the absence of very high temperature regions in the flow. The choice of the Treanor–Marrone coupling parameter U_{TM} (governed in the present study by the value of the uncertain parameter α_U) also has little impact on the flow, both due to the small role of chemical reactions and the more significant role of recombination (the rate of which is independent of the choice of vibrational-chemical coupling) in expanding flows compared to dissociation reactions.

One final aspect that is considered is the choice of vibrational distribution function. The simulations presented used the standard Boltzmann distribution over the vibrational energies, as is commonly done in CFD codes.[3] However, such a description is not entirely rigorous in case when anharmonic vibrational spectra are assumed[37] (as is done in the present work), and the Treanor distribution has to be used instead.[23,37] The issue with the application of the Treanor distribution to expansion flow simulation is the fact that for conditions where $T_v > T$ (which are exactly those that occur in nozzle flows), the distribution becomes non-monotonic: the population of vibrational levels decreases with the vibrational energy only up to a certain level i_*, and then starts increase, which is a non-physical behaviour. Thus, various compound distributions are used instead, with the Treanor distribution cut off at level i_* and continued with some other distribution of the vibrational energy.[5] These can better capture the non-Boltzmann distributions observed in the vibrationally frozen nozzle flows.[30,32,34] In order to estimate the role of the choice of vibrational distribution model, we performed a second set of simulations using the same uncertainty ranges for the relaxation rates and reservoir conditions, but using a compound Treanor–Boltzmann distribution (a Treanor distribution over levels up to i_* continued by a Boltzmann distribution over the higher-lying vibrational states).

At the critical cross-section, the flow is assumed to be in vibrational equilibrium, and thus, at $L = 0$ the choice of the distribution function has no impact on the value of the vibrational temperature at that point; however, as the difference between T_v and T grows, so will the role of the choice of vibrational distribution function. For the condition considered in the current test case, use of the compound Treanor–Boltzmann distribution only slightly affects T_v, leading to a mean value of 3193 K at the nozzle exit, with an uncertainty of ±2.6%. Thus, the difference between the mean results obtained with the two different vibrational distributions differ by approximately 1.1% at the nozzle exit; this lower value (compared to that calculated using the Boltzmann distribution) obtained with the compound distribution is consistent with previous studies on the impact of vibrational distributions on expansion flow simulations.[5,6]

3.2 HEG Expansion

Next, we consider the high-enthalpy case of expansion through the HEG V nozzle.

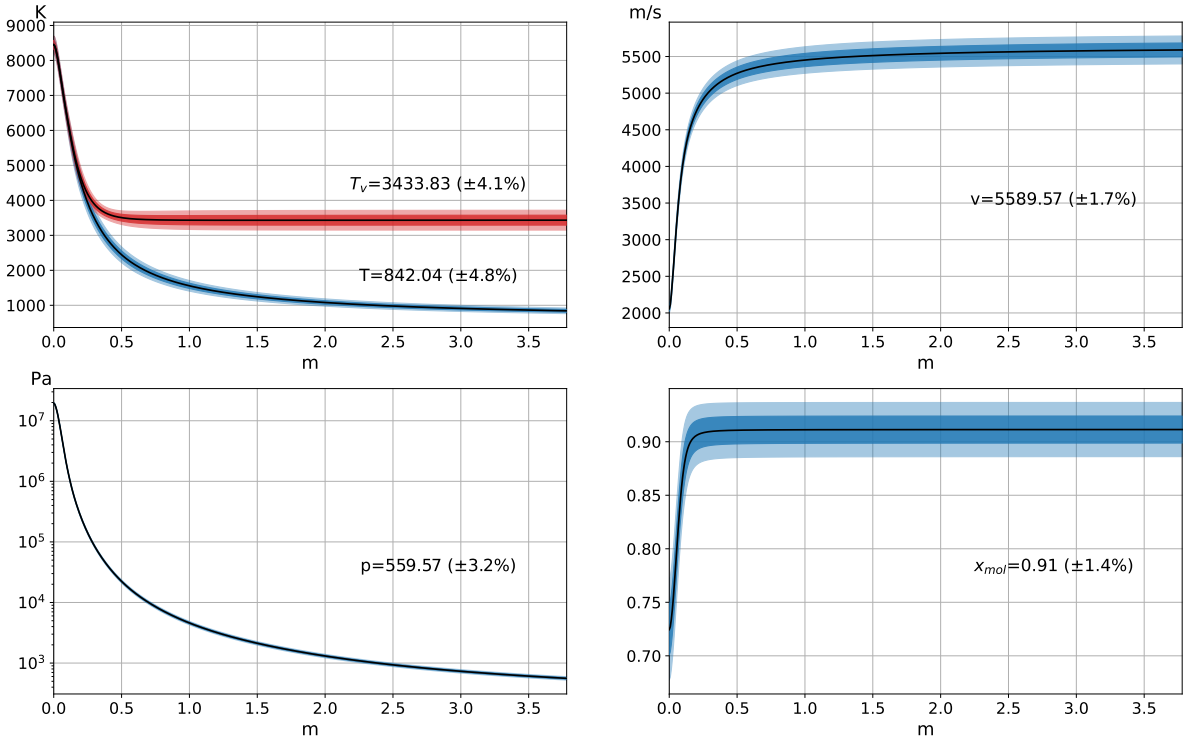

Figure 7: Profiles of temperatures, velocity, pressure, and molecular molar fraction along the nozzle axis. Flow of nitrogen through HEG Nozzle V. Values at nozzle exit expressed explicitly.

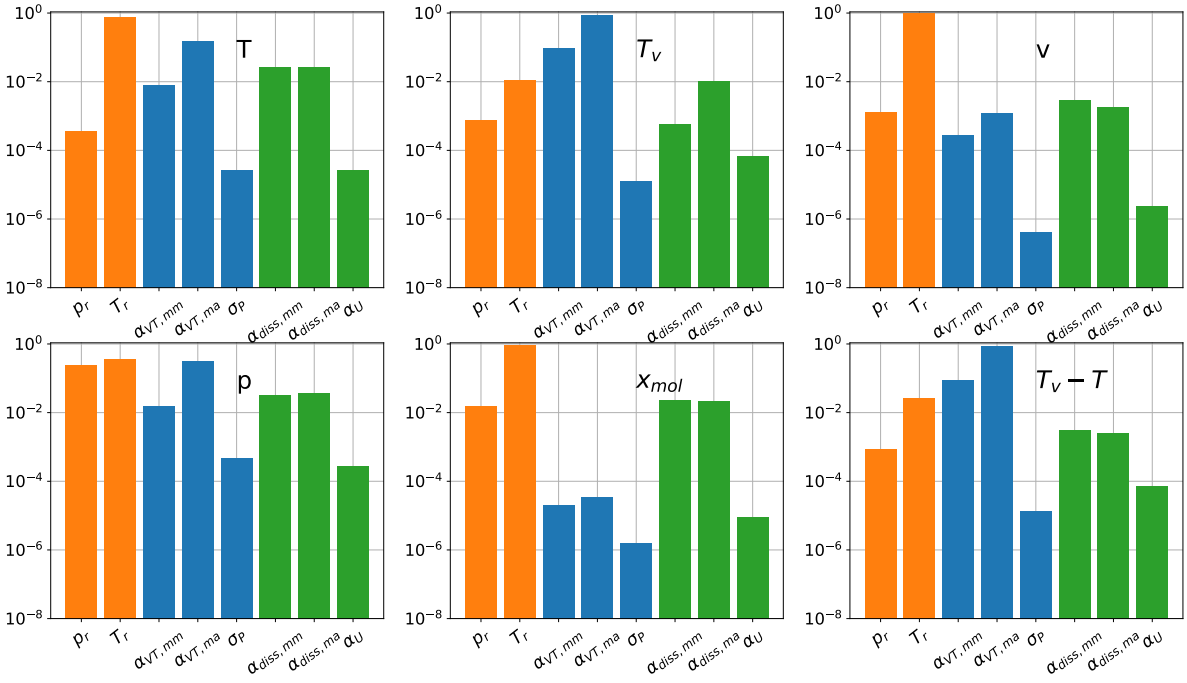

Figure 8: Total Sobol sensitivity indices of flow parameters at nozzle exit with respect to uncertain model parameters. Flow of nitrogen through HEG Nozzle V.

Figure 7 shows the properties (temperature, vibrational temperature, velocity, pressure, and molar fraction of molecules) of a pure nitrogen flow computed along the nozzle center line between the nozzle throat (L = 0 m) and nozzle exit (L = 3.78 m). The Treanor–Marrone dissociation model was used for the simulations. Due to the high reservoir enthalpy and the long nozzle, a much higher degree of non-equilibrium is observed in the flow compared to the NASA EAST test case. The translational and vibrational temperatures exhibit the strongest overall sensitivity (up to 4%), and some variation (1.4%) is also present in the chemical composition of the mixture.

Figure 8 shows the sensitivities of the flow properties with respect to each of the uncertain parameters. Compared to the lower-enthalpy EAST test case, a stronger influence of chemistry is evident, especially on the flow temperature. Furthermore, the higher level of atomic nitrogen in the HEG case leads to collisions with atoms take over the leading sensitivity in the thermal relaxation process. The temperature drops quickly due to the rapid expansion, and thus, the high-temperature Park correction to the vibrational relaxation times has the weakest influence on the flow properties, despite the high temperature in the critical cross-section. As the dominant reaction mechanism in expanding binary flows is recombination, the influence of vibrationally preferential dissociation (described in the model by the parameter α_U governing the U_{TM} vibration-dissociation coupling factor in the Treanor–Marrone model) is also low. Overall, compared to the lower-enthalpy case, the main variation in the flow properties still comes from uncertainties in the reservoir conditions and the vibrational relaxation rates.

Table 1: Flow properties and their uncertainties at nozzle exit for different computational models

	T, K	**T_v, K**	**v, m/s**	**p, Pa**	**x_{mol}**
T.–M., Boltz. VDF	842 (±4.8%)	3434 (±4.1%)	5589 (±1.7%)	560 (±3.1%)	0.91 (±1.4%)
T.–M., T.–B. VDF	842 (±4.7%)	3252 (±3.4%)	5589 (±1.7%)	560 (±3.1%)	0.91 (±1.4%)
P., Boltz. VDF	854 (±4.8%)	3325 (±3.8%)	5594 (±1.7%)	567 (±3.1%)	0.91 (±1.4%)
P., T.–B. VDF	855 (±4.8%)	3171 (±3.2%)	5594 (±1.7%)	567 (±3.1%)	0.91 (±1.4%)
T.–M., Boltz. VDF, with e^-	842 (±4.7%)	3432 (±4.1%)	5590 (±1.7%)	560 (±3.2%)	0.91 (±1.4%)

As the degree of thermal and chemical non-equilibrium in the flow is higher than for the NASA EAST test case considered earlier, a more significant impact of the choice of vibrational distribution function model and vibration-dissociation coupling model can be expected. Therefore, we performed several additional sets of computations: one with the Park dissociation model instead of the Treanor–Marrone model, two with the compound Treanor–Boltzmann distribution instead of the Boltzmann vibrational distribution (using the Treanor–Marrone or the Park dissociation models), and one with additional vibrational relaxation time uncertainty due to electrons produced via ionization using the approximate procedure described in Sec. 2. Since the differences between the results obtained with the different models are not large throughout most of the nozzle, for clarity of presentation, only the values at the nozzle exit (L=3.78 m) are shown in Table 1. The "P." and "T.–M." denote the Park and Treanor–Marrone dissociation models, correspondingly; "Boltz. VDF" and "T.–B. VDF" denote the Boltzmann and compound Treanor–Boltzmann distributions, correspondingly. It is evident that the choice of vibrational distribution and dissociation model has a noticeable effect on the vibrational temperature. The physically superior model for the distribution of vibrational energy levels results in about a 5% lower vibrational temperature predicted at the nozzle exit. But it hardly changes any other flow feature, since the vibrational temperature enters the numerical model directly only via the non-equilibrium dissociation rate, which plays a minor role in the nozzle expansion. The Landau–Teller approach of the vibrational relaxation is driven only by the energy difference and not the temperature difference. Thus, the difference in the vibrational temperature is a different interpretation of the same vibrational energy, for which the equations are solved; this has to be taken into account when comparing with experimental data. The Park dissociation model freezes less vibrataional energy compared to the Treanor–Marrone model and therefore predicts slightly higher translational temperature and velocity at the nozzle exit.

As evidenced by the last line in Table 1, the influence of ionization is very small, as the results differ very slightly from the case with no ionization. As seen from Fig. 7, the region where vibrational non-equilibrium is present begins roughly at temperatures of 4000 K, where the equilibrium electron number density is low, and thus, the presence of electrons has little influence on the vibrational relaxation rate. Freezing of the charged particle recombination might lead to higher electron densities and higher electron temperatures than the ones computed using the equilibrium assumption; a more consistent investigation of the potential impact of ionization is planned for future work. Analysis of the sensitivities of the flow properties with respect to the approximated electron number density parameter $\alpha_{VT,e}$, as depicted on Fig. 9, shows that the impact of the electrons (at least, in the present simplified formulation) is negligibly small.

Analysis of the sensitivities for the case of the Park dissociation model and the compound Treanor–Boltzmann distribution showed the same trends as depicted on Fig. 8, with the main contributors to the flow uncertainty being the

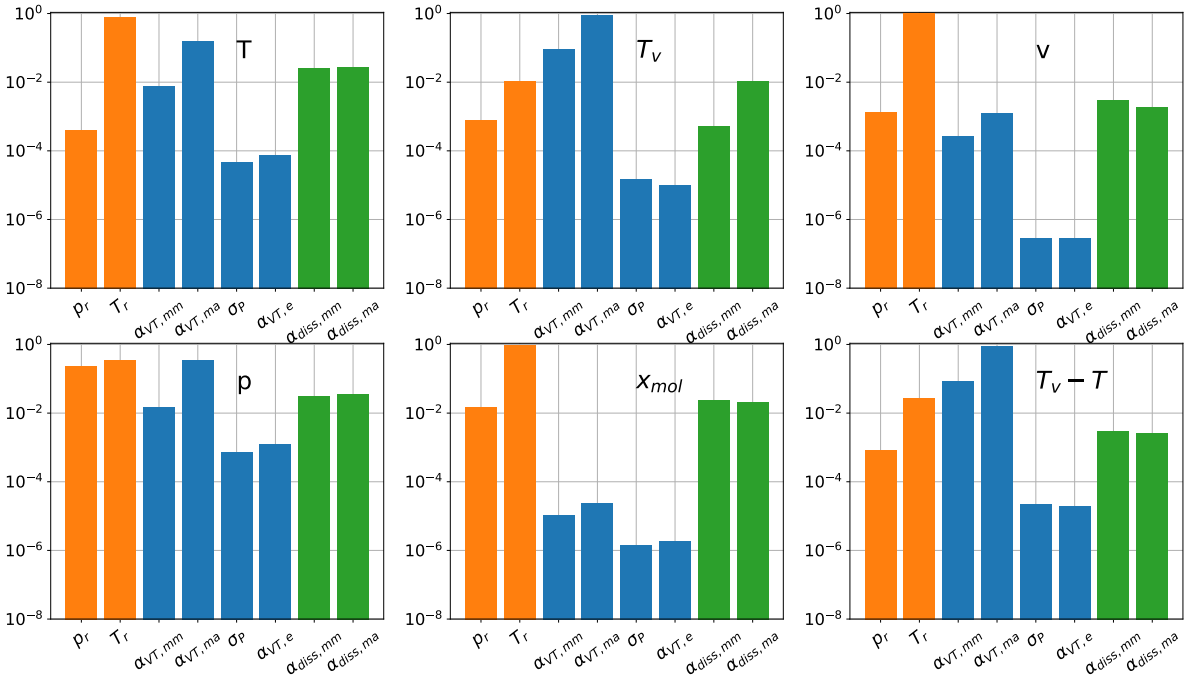

Figure 9: Total Sobol sensitivity indices of flow parameters at nozzle exit with respect to uncertain model parameters. Flow of nitrogen through HEG Nozzle V with equilibrium electron number densities.

uncertainties in the reservoir conditions and vibrational relaxation times.

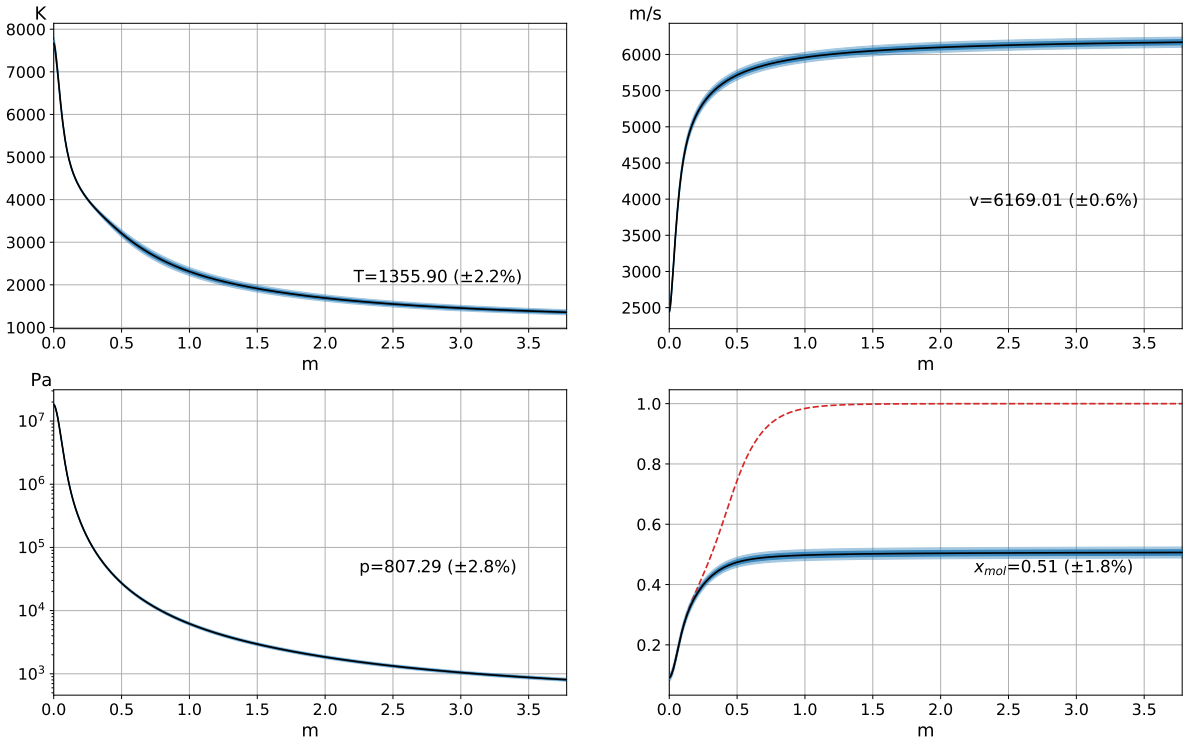

Figure 10: Profiles of temperature, velocity, pressure, and molecular molar fraction along the nozzle axis. Flow of oxygen through HEG Nozzle V. Values at nozzle exit expressed explicitly.

Finally, we consider the same set of reservoir conditions and the same HEG V nozzle, but model a flow of oxygen through the nozzle. Figure 10 shows the flow properties (computed using the Boltzmann vibrational distribution and

Treanor–Marrone dissociation model) along the nozzle axis. Due to the rapid vibrational relaxation of oxygen, the difference between T_v and T remains extremely small (on the order of 10 K) throughout the whole nozzle; therefore, only the temperature is plotted. Since the flow remains in vibrational equilibrium, the equilibrium molar fraction can be computed from the pressure and temperature data throughout the nozzle, this is shown with the dashed red-line on Fig. 10. It can be seen that the chemical composition remains in equilibrium throughout the first 20-25 cm of the nozzle, but further along the nozzle, the chemical reactions freeze rapidly, and the composition becomes strongly non-equilibrium. Due to the very low degree of vibrational non-equilibrium, the choice of vibrational distribution function model or vibrational-dissociation coupling model has little impact on the flow properties.

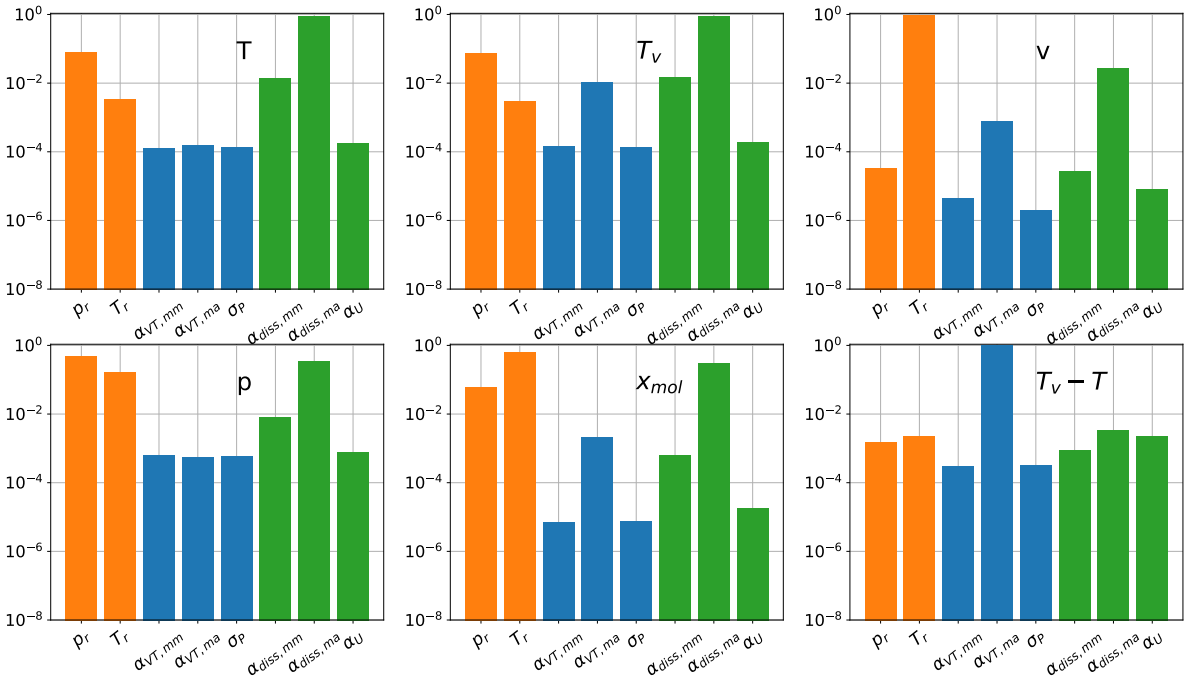

Figure 11: Total Sobol sensitivity indices of flow parameters at nozzle exit with respect to uncertain model parameters. Flow of oxygen through HEG Nozzle V.

Figure 11 shows the total sensitivity indices of the flow parameters with respect to the uncertain model parameters. It can be seen that apart from the reservoir conditions, it is the chemical reaction rates that have the most the influence. Analyzing the sensitivity of the degree of vibrational non-equilibrium, as quantified by $T_v - T$, it is evident that the fast relaxation time of oxygen in collisions with oxygen atoms is the main reason for the almost vibrationally equilibrium flow.

4. Conclusion

In the present work, the methodology for uncertainty quantification and sensitivity analysis of expanding high-enthalpy flows has been presented and applied to binary flows of nitrogen and oxygen for several conditions based on NASA EAST and HEG test conditions. The utilized approach, based on polynomial chaos expansion, allows for global uncertainty quantification/sensitivity analysis study of the join impact of all uncertain model parameters on the flow, whilst requiring relatively little computational effort compared to traditional Monte Carlo methods. Moreover, a parametrization of vibrational relaxation times and chemical reaction rates has been proposed, which reduces the number of model parameters, and allows one to better maintain a physically meaningful range of values.

Numerical studies show that in nitrogen, the main sources of uncertainty in the flow properties at the nozzle exit are uncertainties in the reservoir conditions and vibrational relaxation times, whereas in oxygen, the flow is close to thermal equilibrium and is most sensitive to the chemical reaction rates. Due to the rapid drop in temperature, even in high-enthalpy conditions the flows were found to be very weakly sensitive to high-temperature relaxation time corrections; the impact of the degree of vibration-dissociation coupling was also found to be small. The minor role of the dissociation reaction in expanding flows reduces the choice of Treanor–Marrone or Park preferential dissociation model mainly to the different amount of vibrational energy gained by the recombination of molecules. Due to the

lower vibrational relaxation times for molecule-atom collisions, the role of uncertainty in this relaxation pathway is more significant in both nitrogen and oxygen flows when sufficient atoms are present. For the higher-enthalpy conditions, the choice of vibrational distribution model and vibration-dissociation coupling model was found to have a noticeable effect on the vibrational temperature at the nozzle exit. A preliminary analysis of the potential influence of flow ionization on the flow (via electron-impact vibrational relaxation) showed that it has little influence, at least within the simplified approach utilized in the present work.

Simulations of oxygen flows through the HEG nozzle showed that the flow remains in vibrational equilibrium throughout the nozzle due to the fast vibrational relaxation via molecule-atom collisions; a strong degree of chemical non-equilibrium is present throughout the flow. Sensitivity analysis studies show that the flow parameters are mostly influenced by the reservoir conditions and chemical reaction rates. The study is planned to be extended to a wider range of reservoir enthalpies, as well as to air flows.

5. Acknowledgments

Georgii Oblapenko acknowledges the funding provided by the Alexander von Humboldt foundation for his stay as a guest researcher at the German Aerospace Center (DLR).

References

[1] André, P. 1997. Numerical method and composition at and out of chemical equilibrium in a multitemperature plasma. application to a pure nitrogen plasma. *Contrib. Plasma Phys.*, 37(1):23–40.

[2] Brune, A., T. West IV, S. Hosder, and K. Edquist. 2015. Uncertainty analysis of Mars entry flows over a hypersonic inflatable aerodynamic decelerator. *J. Spacecr. Rockets*, 52(3):776–788.

[3] Candler, G., and R. MacCormack. 1991. Computation of weakly ionized hypersonic flows in thermochemical nonequilibrium. *J. Thermophys. Heat Transfer*, 5(3):266–273.

[4] Chaudhry, R., and G. Candler. 2019. Statistical analyses of quasiclassical trajectory data for air dissociation. In *AIAA Scitech 2019 Forum*, paper 0789.

[5] Chikhaoui, A., E. Nagnibeda, E. Kustova, and T. Alexandrova. 2001. Modeling of dissociation–recombination in nozzles using strongly non-equilibrium vibrational distributions. *Chem. Phys.*, 263(1):111–126.

[6] Colonna, G., I. Armenise, D. Bruno, and M. Capitelli. 2006. Reduction of state-to-state kinetics to macroscopic models in hypersonic flows. *J. Thermophys. Heat Transfer*, 20(3):477–486.

[7] Cortesi, A., P. Constantine, T. Magin, and P. Congedo. 2020. Forward and backward uncertainty quantification with active subspaces: application to hypersonic flows around a cylinder. *J. Comput. Phys.*, 407:109079.

[8] Cutler, A., G. Magnotti, L. Cantu, E. Gallo, P. Danehy, R. Baurle, R. Rockwell, C. Goyne, and J. McDaniel. 2012. Measurement of vibrational nonequilibrium in a supersonic freestream using dual-pump CARS. In *28th Aerodynamic Measurement Technology, Ground Testing, and Flight Testing Conference including the Aerospace T&E Days Forum*, paper 3199.

[9] Feinberg, J., and H. Langtangen. 2015. Chaospy: An open source tool for designing methods of uncertainty quantification. *J. Comput. Sci.*, 11:46–57.

[10] Gimelshein, S., and I. Wysong. 2021. Nonequilibrium effects in high enthalpy gas flows expanding through nozzles. *Phys. Fluids*, 33(10):106104.

[11] Gimelshein, S., I. Wysong, A. Fangman, D. Andrienko, O. Kunova, E. Kustova, F. Morgado, C. Garbacz, M. Fossati, and K. Hanquist. 2022. Kinetic and continuum modeling of high-temperature air relaxation. *J. Thermophys. Heat Transfer*, pages 1–23.

[12] Gu, S., J. Hao, and C. Wen. 2022. State-specific study of air in the expansion tunnel nozzle and test section. *AIAA Journal*, pages 1–15.

[13] Gülhan, A., B. Esser, U. Koch, M. Fischer, E. Magens, and V. Hannemann. 2018. Characterization of high-enthalpy-flow environment for ablation material tests using advanced diagnostics. *AIAA Journal*, 56(3):1072–1084.

[14] Gupta, R., J. Yos, R. Thompson, and K. Lee. 1990. A review of reaction rates and thermodynamic and transport properties for an 11-species air model for chemical and thermal nonequilibrium calculations to 30000 K.

[15] Hannemann, K., J. Martinez Schramm, A. Wagner, and G. Ponchio Camillo. 2018. The high enthalpy shock tunnel Göttingen of the German aerospace center (DLR). *Journal of large-scale research facilities JLSRF*, 4(A133):1–14.

[16] K Higdon, K., D. Goldstein, and P. Varghese. 2018. Sensitivity analysis of Direct Simulation Monte Carlo parameters for ionizing hypersonic flows. *J. Thermophys. Heat Transfer*, 32(1):90–102.

[17] Kieweg, S., J. Ray, V. Weirs, B. Carnes, D. Dinzl, B. Freno, M. Howard, E. Phipps, W. Rider, and T. Smith. 2019. Validation assessment of hypersonic double-cone flow simulations using uncertainty quantification, sensitivity analysis, and validation metrics. In *AIAA Scitech 2019 Forum*, paper 2278.

[18] Kustova, E., E. Nagnibeda, G. Oblapenko, A. Savelev, and I. Sharafutdinov. 2016. Advanced models for vibrational–chemical coupling in multi-temperature flows. *Chem. Phys.*, 464:1–13.

[19] Kustova, E., and A. Savelev. 2021. Generalized model for state-resolved chemical reaction rate coefficients in high-temperature air. In *Journal of Physics: Conference Series*, volume 1959, paper 012033. IOP Publishing.

[20] Kustova, E., and G. Oblapenko. 2016 Mutual effect of vibrational relaxation and chemical reactions in viscous multitemperature flows. *Phys. Rev. E*, 93(3):033127.

[21] Lee, J.-H. 1993. Electron-impact vibrational relaxation in high-temperature nitrogen. *J. Thermophys. Heat Transfer*, 7(3):399–405, 1993.

[22] Marrone, P., and C. Treanor. 1963. Chemical relaxation with preferential dissociation from excited vibrational levels. *Phys. Fluids*, 6(9):1215–1221.

[23] Nagnibeda, E., and E. Kustova. *Non-equilibrium reacting gas flows: kinetic theory of transport and relaxation processes*. Springer Science & Business Media, 2009.

[24] Neely A., R. Stalker, and A. Paull. 1991. High enthalpy, hypervelocity flows of air and argon in an expansion tube. *Aeronaut. J.*, 95(946):175–186.

[25] Oblapenko, G. 2018. Calculation of vibrational relaxation times using a kinetic theory approach. *J. Phys. Chem. A.*, 122(50):9615–9625.

[26] Oblapenko, G., E. Kustova, K. Hannemann, and V. Hannemann. 2019. Assessment of recent thermo-chemical relaxation models using the DLR-TAU code. In *AIP Conference Proceedings*, volume 2132, page 140006. AIP Publishing LLC.

[27] Palma, P., P. Danehy, and A. Houwing. 2003. Fluorescence imaging of rotational and vibrational temperature in shock-tunnel nozzle flow. *AIAA Journal*, 41(9):1722–1732.

[28] Park, C. 1993. Review of chemical-kinetic problems of future NASA missions. I-Earth entries. *J. Thermophys. Heat Transfer*, 7(3):385–398.

[29] Park, C. and S.-H. Lee. 1995. Validation of multitemperature nozzle flow code. *J. Thermophys. Heat Transfer*, 9(1):9–16.

[30] Ruffin, S. 1995. Prediction of vibrational relaxation in hypersonic expanding flows part 2: Results. *J. Thermophys. Heat Transfer*, 9(3):438–445.

[31] Scanlon., T., C. White, M. Borg, R. Palharini, E. Farbar, I. Boyd, J. Reese, and R. Brown. 2015. Open-source direct simulation Monte Carlo chemistry modeling for hypersonic flows. *AIAA Journal*, 53(6):1670–1680.

[32] Sharma, S., S. Ruffin, W. Gillespie, and S. Meyer. 1993. Vibrational relaxation measurements in an expanding flow using spontaneous Raman scattering. *J. Thermophys. Heat Transfer*, 7(4):697–703.

[33] Shoev, G., G. Oblapenko, O. Kunova, M. Mekhonoshina, and E. Kustova. 2018. Validation of vibration-dissociation coupling models in hypersonic non-equilibrium separated flows. *Acta Astronautica*, 144:147–159.

[34] Singh, N. and T. Schwartzentruber. 2020. Non-boltzmann vibrational energy distributions and coupling to dissociation rate. *J. Chem. Phys.*, 152(22):224301.

[35] Smith, R. 2013. *Uncertainty quantification: theory, implementation, and applications*, volume 12. SIAM.

[36] Streicher, J., A. Krish, and R. Hanson. 2021. Coupled vibration-dissociation time-histories and rate measurements in shock-heated, nondilute O2 and O2–Ar mixtures from 6000 to 14 000 K. *Phys. Fluids*, 33(5):056107.

[37] Treanor, C., J. Rich, and R. Rehm. 1968. Vibrational relaxation of anharmonic oscillators with exchange-dominated collisions. *J. Chem. Phys.*, 48(4):1798–1807.

[38] Venturi, S. 2021. *Machine learning and uncertainty quantification framework for predictive ab initio Hypersonics*. PhD thesis, University of Illinois at Urbana-Champaign.

[39] Wang, X., C. Yan, S. Ju, Y. Zheng, and J. Yu. 2017. Uncertainty analysis of laminar and turbulent aeroheating predictions for Mars entry. *Int. J. Heat Mass Tran.*, 112:533–543.

[40] Weaver, A., A. Alexeenko, R. Greendyke, and J. Camberos. 2011. Flowfield uncertainty analysis for hypersonic computational fluid dynamics simulations. *J. Thermophys. Heat Transfer*, 25(1):10–20.

[41] West IV, T., and S. Hosder. 2015. Uncertainty quantification of hypersonic reentry flows with sparse sampling and stochastic expansions. *J. Spacecr. Rockets*, 52(1):120–133.

[42] Winter, M., C. Srinivasan, R. Charnigo, and D. Prabhu. 2018. Spectroscopic analysis of nonequilibrium excited state chemistry in a NASA arc jet. *J. Thermophys. Heat Transfer*, 32(4):1088–1098.

[43] Zheng, Y., C. Yan, and Y. Zhao. 2020. Uncertainty and sensitivity analysis of inflow parameters for HyShot II scramjet numerical simulation. *Acta Astronautica*, 170:342–353.